Title:

Expression dynamics of ARGONAUTE proteins during meiosis in Arabidopsis

Authors and affiliation:

Cecilia Oliver and German Martinez.

Department of Plant Biology, Uppsala BioCenter, Swedish University of Agricultural Sciences and Linnean Center for Plant Biology, Uppsala, Sweden

Corresponding authors:

Cecilia Oliver: cecilia.oliver.velasco@slu.se

German Martinez: german.martinez.arias@slu.se

ORCID information:

Cecilia Oliver: 0000-0002-5231-7910

German Martinez: 0000-0002-5215-0866

Abstract

Meiosis is a specialized cell division that is key for reproduction and genetic diversity in sexually reproducing plants. Recently, different RNA silencing pathways have been proposed to carry a specific activity during meiosis, but the pathways involved during this process remain unclear. Here, we explored the subcellular localization of different ARGONAUTE (AGO) proteins, the main effectors of RNA silencing, during male meiosis in *Arabidopsis thaliana* using immunolocalizations with commercially available antibodies. We detected the presence of AGO proteins associated with posttranscriptional gene silencing (AGO1, 2 and 5) in the cytoplasm or the nucleus, while AGOs associated with transcriptional gene silencing (AGO4 and 9) localized exclusively in the nucleus. These results indicate that the localization of different AGOs correlates with their predicted roles at the transcriptional and posttranscriptional levels and provide an overview of their timing and potential role during meiosis.

Introduction

Meiosis is a special type of cell division where one round of DNA synthesis is followed by two rounds of cell division, segregating homologous chromosomes during the first division and sister chromatids at the second division (Marston et al. 2004, Mercier et al. 2015). This process is key for the production of gametes and the reshuffling of the genetic information during sexual reproduction (Bolcun-Filas et al. 2018). The mechanisms regulating meiosis have been widely studied at the cellular, genetic, and molecular levels in a variety of organisms. In plants, more than 90 genes have been identified comprising

different meiotic processes that include double-strand break (DSB) formation, chromosome segregation or meiotic recombination (Huang et al. 2019a). Intriguingly, in the recent years it has been revealed that several of these processes involve the RNA silencing machinery (Oliver et al. 2016, Underwood et al. 2018, Wei et al. 2012). Different RNA silencing pathways are active during meiosis (Huang et al. 2020, Huang, et al. 2019a, Yelina et al. 2015). The miRNA affects chromatin condensation and the number of chiasmas, while the RNA-directed DNA methylation (RdDM) pathways affects chromatin condensation, the number of chiasmas and chromosome segregation (Oliver et al. 2017, Oliver, et al. 2016). Moreover, the RdDM pathway protects euchromatic regions from meiotic recombination (Yelina, et al. 2015). Additionally, *Arabidopsis* a non-canonical RNA silencing pathway plays a role in double-strand break repair (Wei, et al. 2012). Moreover, meiocyte-specific sRNAs between 23-24 nts are positively correlated with genes that have a meiocyte-preferential expression pattern (Huang, et al. 2019a), which could correlate with the observed role of DNA methylation in the regulation of gene expression in meiocytes (Walker et al. 2018). ARGONAUTE (AGO) proteins are the effectors of the different RNA silencing pathways and have dedicated members that act at the posttranscriptional or transcriptional levels. Here, we analyze the subcellular localization of the main AGO proteins in Arabidopsis during the different meiosis stages, which provides a confirmation of their activity during this process.

Materials and Methods

Plant material

Plants used for immunolocalization analysis were grown in a phytotron under long day conditions (16-hour light/8-hour dark photoperiod), at 24-25 °C and 45% relative humidity.

Bioinformatic analysis

sRNA data was downloaded from the SRA repository project number PRJNA510650 (Huang et al. 2019b). sRNA alignments were performed using bowtie (Langmead et al. 2009) with the following parameters –t –v2 that allows 2 mismatches to the alignments. Alignment files were subsequently analyzed in Galaxy (Afgan et al. 2018). For sRNA categorization as miRNAs, sRNA libraries were aligned to individual indexes generated for each genomic category and compared total sRNAs mapping to the TAIR10 chromosome sequences. The miRbase version 22.1 (https://www.mirbase.org/) was used for miRNA alignments (Kozomara et al. 2019). Transcriptomic data corresponds to the CATMA arrays data from GEO accessions GSE10229 and GSE13000 (Libeau et al. 2011). CATMA array data was extracted using the CATdb database (http://urgv.evry.inra.fr/cgi-bin/projects/CATdb/catdb_index.pl) were normalized data was extracted for both GSE10229 (http://urgv.evry.inra.fr/cgi-bin/projects/CATdb/consult_expce.pl?experiment_id=195) and GSE13000 (http://urgv.evry.inra.fr/cgi-bin/projects/CATdb/consult_expce.pl?experiment_id=46).

Cytology

Immunolocalization on meiotic nuclei were carried out by squash technique as was previously described by Manzanero et al. (2000) with some modifications (Oliver et al.,

2013). Two bioreplicates constituted by young flower buds from five different plants, were analyzed. Young flower buds were fixed for 20 min in freshly prepared 4 % (w/v) paraformaldehyde, 0.1 % (v/v) Triton X-100 in phosphate-buffered saline (PBS, pH 7.3). Flower buds were then washed at room temperature for 30 min in PBS that was changed twice. Buffer was removed before incubation at 37ºC during 20–40 min with an enzyme mixture of 1 % pectinase, 1 % cellulase and 1 % cytohelicase (w/v) (Sigma), dissolved in PBS. Buds, immersed in a small volume of PBS, were transferred to slides with a Pasteur pipette, macerated with a needle and squashed between a glass slide and cover slip. After freezing in liquid nitrogen, the cover slips were removed and the slides were transferred immediately into PBS. Prior to immunostaining experiments the slides were washed twice in PBS, 0.1 % (v/v) Triton X-100 for 5 min each. To avoid non-specific antibody binding, slides were incubated for 30 min in PBS with 1 % BSA (w/v) and 0.1 % Triton X-100 at room temperature. The incubation with the primary antibody was carried out in a humidified chamber. The primary antibodies used were rabbit anti-AGO1 (1:200 AS09 527), -AGO2 (1:100, AS13 2682), -AGO5 (1:100, AS10 671), -AGO4 (1:100, AS09 617), -AGO6 (1:50, AS10 672), -AGO9 (1:100, AS10 673) and -AGO10 (1:50, AS15 3071) antibodies from Agrisera. All the primary antibodies were diluted in PBS, 1 % BSA, 0.1 % Triton X-100. After overnight incubation at 4ºC and washing for 15 min in PBS with 0.1 % Triton X-100, the slides were incubated for 1 h at room temperature with goat anti-rabbit IgG H&L Alexa Fluor 568 conjugated (1:200; ab175471; Abcam) diluted in 1 % BSA, 0.1 % Triton X-100 in PBS. Slides were then washed in PBS, 0.1 % Triton X-100, before they were stained the DAPI, 1 µg/ml during 20-30 min and finally mounting with antifading medium (0.2% n-propyl Gallete, 0.1% DMSO, 90% glycerol in PBS). Fluorescent signals

were observed using an epifluorescence microscope Zeiss AxioScope A1. Images were captured with AxioCam ICc5 camera and were analyzed and processed with ImageJ and Affinity Photo software.

Results

To discern the level of expression of RNA silencing components in meiocytes, we analyzed their expression from publicly available microarray datasets (Libeau, et al. 2011) (Figure 1 and Supplementary Methods). Overall, several components from the RNA silencing pathways were preferentially expressed in meiocytes compared to somatic tissues (Figure 1A), including the AGO proteins AGO4, 5 and 10, the Dicer-like (DCL) proteins DCL1, 3 and 4 or the sRNA methyltransferase HEN1. This indicated that different PTGS (AGO5, DCL1 and DCL4) and TGS (AGO4 and DCL3) pathways might be especially active during meiosis. Previous analysis (Huang, et al. 2019a) have shown that TE-derived sRNAs accumulate to relatively high levels in meiocytes and that certain miRNAs like miR845 are active before the microspore stage (Borges et al. 2018). Although miRNAs were not globally enriched in meiocytes (Figure 1B), several miRNAs were strongly upregulated including miR839, miR780.2, miR780.1, miR157, miR172, miR166 and miR860, which are important regulators of several transcription factor families (Figure 1C, Supplementary Figure 1 and Supplementary Table 2). In summary, transcriptomic and sRNA sequencing analysis supported the notion that the RNA silencing machinery might have a meiocyte-specific activity.

Although transcriptomic analysis is important to infer the activity of the different RNA silencing pathways in meiocytes, this analysis provides a steady image of this tissue and ignores, for example, its dynamism during meiosis. To understand the subcellular localization and dynamics of the different AGO proteins during meiosis, we performed immunolocalizations of the AGO proteins that had commercially available antibodies (Agrisera, AGO1, 2, 4, 5, 6, 9 and 10, Figure 2 and Supplementary Methods). During meiosis all AGOs but AGO6 and AGO10 could be detected. In detail, AGO1 and its paralogs AGO2 and AGO5 displayed a similar localization and expression pattern during the first meiotic stages (Figure 2A, 2B, 2C). The three proteins were located mainly in the cytoplasm, similar to their localization in somatic tissues (Bologna et al. 2018, Ye et al. 2012). From the leptotene to the diplotene stage these three AGO proteins formed cytoplasmic granules (Figure. 2A1, 2B1, 2C1). In somatic tissues, cytoplasmic bodies are involved in the degradation and translation arrest of mRNAs (Maldonado-Bonilla 2014). In mammals, AGO proteins localize in P-bodies where they mediate the translational repression of their target mRNAs (Liu et al. 2005). The localization pattern observed for AGO1, 2 and 5 might indicate a similar role of RNA silencing in the posttranscriptional regulation of mRNAs, a process that is known to take place in other organisms like mammals (Yao et al. 2015).

Despite the similarities between the accumulation during meiosis, AGO1, 2 and 5, they showed differences in their dynamics during meiosis. For example, AGO1 condensates around the nuclear envelope at diplotene (Figure 2A4) but after this stage, it showed a disperse accumulation (Figure 2A5). This location during cell division could be related

with the known AGO1 association with the endoplasmic reticulum (Li et al. 2013), as when the nuclear envelope disassembles it reorganizes in vacuoles around the bivalents (Marston, et al. 2004, Mercier, et al. 2015). AGO5 displayed a similar pattern of subcellular localization to AGO1, although its localization at cytoplasmic bodies disappeared at diplotene (Figure 2B4). On the other hand, AGO2 showed a dual localization in the cytoplasm and in the nucleus (Figure 2C1-4) and was not detectable after metaphase I (Figure 2C5-6). Both its nucleocytoplasmic localization and timing of expression are in line with its known role in double strand break (DSB) repair, which takes place during the first meiotic stages (Oliver et al. 2014, Wei, et al. 2012). Nevertheless, AGO2 expression pattern was recapitulated after the second meiotic division (Figure 2C7), indicating that it might serve other roles in parallel to its function in DSB repair during meiosis.

On the other hand, the TGS/RdDM-associated AGO proteins, AGO4 and AGO9, were located in the nuclei during all meiotic stages (Figure 2D and E). Exceptionally, at metaphase I, when the nuclear envelope dissolves, both proteins showed a dispersed accumulation. This is in accordance with the known role of the RdDM pathway in regulating DNA methylation during meiosis (Walker, et al. 2018). Meiocytes have the lowest CHH methylation values of all the reproductive nuclei analyzed, but its activity is needed for the regulation of gene expression (Walker, et al. 2018). We detected a low accumulation of AGO4 and 9 after metaphase I (Figure 2D5-6 and 2E5-6), which might partially cause this reduction in CHH methylation. Interestingly, we observed that AGO9 displayed a localization pattern compatible with a preference for heterochromatic regions

at pachytene. This localization might explain the known role of AGO9 on the dissolution of interlocks during meiosis (Oliver, et al. 2014).

Discussion

In summary, our results provide an overview of the subcellular localization, timing and potential role of different RNA silencing pathways during meiosis. Furthermore, our work complements previous analysis that analyzed RNA silencing activity in meiocytes, and opens the door for future molecular analysis of the specific role of AGO proteins during specific meiosis stages, which are technically challenging at the moment.

Author contribution statement: C.O and G.M. design the experiments and wrote the manuscript. C.O. performed the experiments and analyzed the data. G.M. analyzed the bioinformatic data.

Acknowledgements

The authors thank SLU, the Carl Tryggers Foundation (CTS 17-305 and CTS 18-251), the Swedish Research Council (VR 2016-05410) and the Knut and Alice Wallenberg Foundation (KAW 2019-0062) for supporting research in the Martinez group. The data handling was enabled by resources provided by the Swedish National Infrastructure for Computing (SNIC) at UPPMAX partially funded by the Swedish Research Council through grant agreement no. 2018-05973.

References:

Afgan E, Baker D, Batut B, van den Beek M, Bouvier D, Čech M, Chilton J, Clements D, Coraor N, Grüning BA, Guerler A, Hillman-Jackson J, Hiltemann S, Jalili V, Rasche H, Soranzo N, Goecks J, Taylor J, Nekrutenko A, Blankenberg D (2018) The Galaxy platform for accessible, reproducible and collaborative biomedical analyses: 2018 update. Nucleic Acids Research 46:W537-W544

Bolcun-Filas E, Handel MA (2018) Meiosis: the chromosomal foundation of reproduction. Biol Reprod 99:112-126

Bologna NG, Iselin R, Abriata LA, Sarazin A, Pumplin N, Jay F, Grentzinger T, Dal Peraro M, Voinnet O (2018) Nucleo-cytosolic Shuttling of ARGONAUTE1 Prompts a Revised Model of the Plant MicroRNA Pathway. Mol Cell 69:709-719 e705

Borges F, Parent JS, van Ex F, Wolff P, Martinez G, Kohler C, Martienssen RA (2018) Transposon-derived small RNAs triggered by miR845 mediate genome dosage response in Arabidopsis. Nat Genet 50:186-192

Huang J, Wang C, Li X, Fang X, Huang N, Wang Y, Ma H, Wang Y, Copenhaver GP (2020) Conservation and Divergence in the Meiocyte sRNAomes of Arabidopsis, Soybean, and Cucumber. Plant Physiol 182:301-317

Huang J, Wang C, Wang H, Lu P, Zheng B, Ma H, Copenhaver GP, Wang Y (2019a) Meiocyte-Specific and AtSPO11-1-Dependent Small RNAs and Their Association with Meiotic Gene Expression and Recombination. Plant Cell 31:444-464

Huang JY, Wang C, Wang HF, Lu PL, Zheng BL, Ma H, Copenhaver GP, Wang YX (2019b) Meiocyte-Specific and AtSPO11-1-Dependent Small RNAs and Their

Association with Meiotic Gene Expression and Recombination. Plant Cell 31:444-464

Kozomara A, Birgaoanu M, Griffiths-Jones S (2019) miRBase: from microRNA sequences to function. Nucleic Acids Research 47:D155-D162

Langmead B, Trapnell C, Pop M, Salzberg SL (2009) Ultrafast and memory-efficient alignment of short DNA sequences to the human genome. Genome Biol 10:R25

Li S, Liu L, Zhuang X, Yu Y, Liu X, Cui X, Ji L, Pan Z, Cao X, Mo B, Zhang F, Raikhel N, Jiang L, Chen X (2013) MicroRNAs inhibit the translation of target mRNAs on the endoplasmic reticulum in Arabidopsis. Cell 153:562-574

Libeau P, Durandet M, Granier F, Marquis C, Berthome R, Renou JP, Taconnat-Soubirou L, Horlow C (2011) Gene expression profiling of Arabidopsis meiocytes. Plant Biol (Stuttg) 13:784-793

Liu J, Valencia-Sanchez MA, Hannon GJ, Parker R (2005) MicroRNA-dependent localization of targeted mRNAs to mammalian P-bodies. Nat Cell Biol 7:719-723

Maldonado-Bonilla LD (2014) Composition and function of P bodies in Arabidopsis thaliana. Front Plant Sci 5:201

Manzanero S, Arana P, Puertas MJ, Houben A (2000) The chromosomal distribution of phosphorylated histone H3 differs between plants and animals at meiosis. Chromosoma 109:308-317

Marston AL, Amon A (2004) Meiosis: cell-cycle controls shuffle and deal. Nat Rev Mol Cell Biol 5:983-997

Mercier R, Mezard C, Jenczewski E, Macaisne N, Grelon M (2015) The molecular biology of meiosis in plants. Annu Rev Plant Biol 66:297-327

Oliver C, Pradillo M, Corredor E, Cuñado N (2013) The dynamics of histone H3 modifications is species-specific in plant meiosis. Planta 238:23-33

Oliver C, Pradillo M, Jover-Gil S, Cunado N, Ponce MR, Santos JL (2017) Loss of function of Arabidopsis microRNA-machinery genes impairs fertility, and has effects on homologous recombination and meiotic chromatin dynamics. Sci Rep 7:9280

Oliver C, Santos JL, Pradillo M (2014) On the role of some ARGONAUTE proteins in meiosis and DNA repair in Arabidopsis thaliana. Frontiers in Plant Science 5

Oliver C, Santos JL, Pradillo M (2016) Accurate Chromosome Segregation at First Meiotic Division Requires AGO4, a Protein Involved in RNA-Dependent DNA Methylation in Arabidopsis thaliana. Genetics 204:543-553

Underwood CJ, Choi K, Lambing C, Zhao X, Serra H, Borges F, Simorowski J, Ernst E, Jacob Y, Henderson IR, Martienssen RA (2018) Epigenetic activation of meiotic recombination near Arabidopsis thaliana centromeres via loss of H3K9me2 and non-CG DNA methylation. Genome Res 28:519-531

Walker J, Gao H, Zhang J, Aldridge B, Vickers M, Higgins JD, Feng X (2018) Sexual-lineage-specific DNA methylation regulates meiosis in Arabidopsis. Nat Genet 50:130-137

Wei W, Ba Z, Gao M, Wu Y, Ma Y, Amiard S, White CI, Rendtlew Danielsen JM, Yang YG, Qi Y (2012) A role for small RNAs in DNA double-strand break repair. Cell 149:101-112

Yao CC, Liu Y, Sun M, Niu MH, Yuan QQ, Hai YA, Guo Y, Chen Z, Hou JM, Liu Y, He ZP (2015) MicroRNAs and DNA methylation as epigenetic regulators of mitosis, meiosis and spermiogenesis. Reproduction 150:R25-R34

Ye R, Wang W, Iki T, Liu C, Wu Y, Ishikawa M, Zhou X, Qi Y (2012) Cytoplasmic assembly and selective nuclear import of Arabidopsis Argonaute4/siRNA complexes. Mol Cell 46:859-870

Yelina NE, Lambing C, Hardcastle TJ, Zhao X, Santos B, Henderson IR (2015) DNA methylation epigenetically silences crossover hot spots and controls chromosomal domains of meiotic recombination in Arabidopsis. Genes Dev 29:2183-2202

Figure legends:

Figure 1. Analysis of the expression in meiocytes of different RNA silencing and epigenetic pathways components and analysis of miRNA accumulation in meiocytes. A. Heat map of the expression values of RNA silencing and epigenetic pathways components in meiocyte microarray experiments. Expression values are represented as the normalized log2 ratio of the comparison meiocyte/control tissue. **B.** Global accumulation of miRNAs in leaves and meiocytes samples from public datasets normalized to reads per million. **C.** Accumulation values of miRNAs enriched in meiocyte sRNA libraries. Enrichment was considered only for miRNAs accumulating more than 2-fold in meiocytes and with a p-value<0.05.

Figure 2. Immunolocalization of AGO1 (A), AGO5 (B), AGO2 (C), AGO4 (D) and AGO9 (E) at different representative meiotic stages in Arabidopsis meiocytes. Leptotene (A1, B1, C1, D1, E1); Zygotene (A2, B2, C2, D2, E2); Pachytene (A3, B3, C3, D3, E3); Diplotene (A4, B4, C4, D4, E4); Diakinesis (B5), Metaphase I (A5, C5, D5, E5)

285 Prophase II (A6, B6, D6, E6); Metaphase II (C6); Tetrad (A7, B7, C7, D7, E7).
286 Immunostaining with antibodies is shown in red, counterstaining with DAPI is shown in
287 grey. Bar indicates 10 μm.

288

289 **Supplementary Figure 1.** Predicted and confirmed targets of miRNA families
290 significantly upregulated in meiocytes.

291

292 **Supplementary Table 1.** Raw values of normalized log2-ratio expression values for
293 selected genes in meiocytes microarray data.

294

295 **Supplementary Table 2.** Raw values of miRNA accumulation in meiocytes and leaf
296 sRNA libraries.

Figure 1

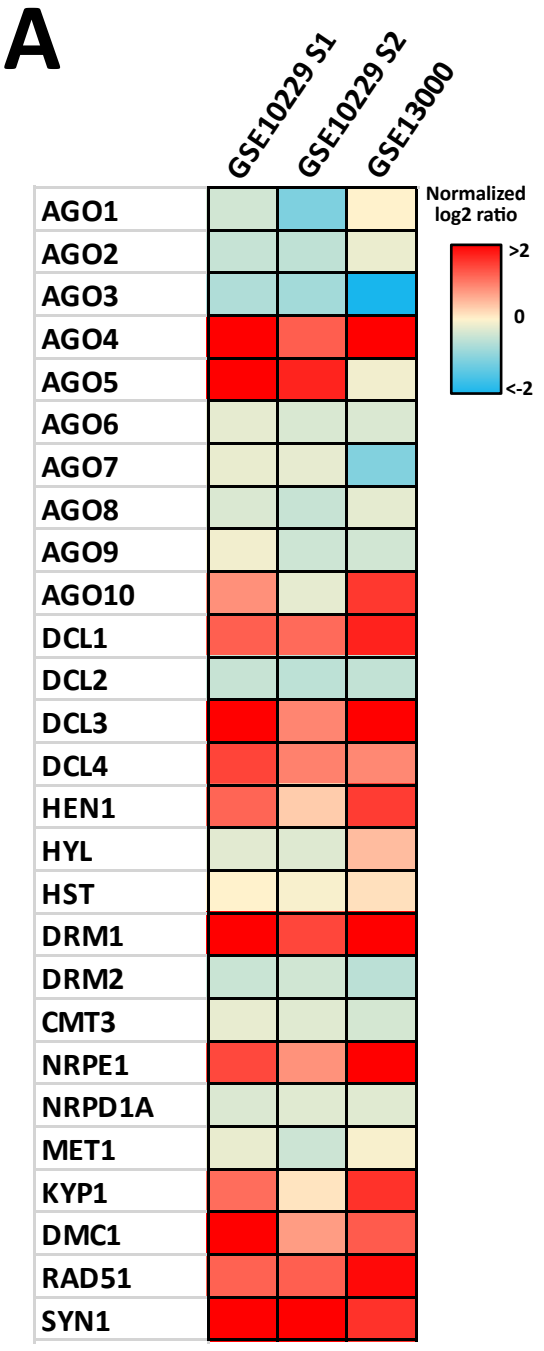
A
GSE10229 S1
GSE10229 S2
GSE13000
Normalized log2 ratio
>2
0
<-2
AGO1
AGO2
AGO3
AGO4
AGO5
AGO6
AGO7
AGO8
AGO9
AGO10
DCL1
DCL2
DCL3
DCL4
HEN1
HYL
HST
DRM1
DRM2
CMT3
NRPE1
NRPD1A
MET1
KYP1
DMC1
RAD51
SYN1

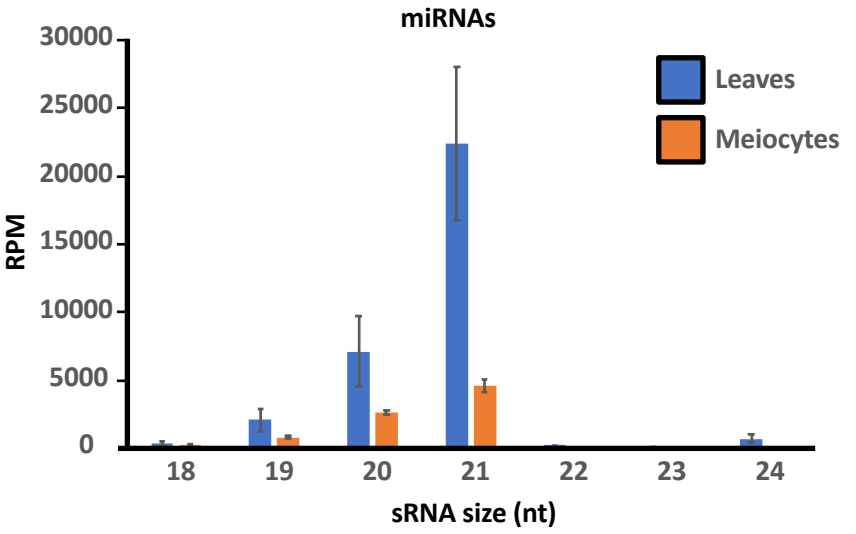
B
miRNAs
Leaves
Meiocytes
RPM
30000
25000
20000
15000
10000
5000
0
18
19
20
21
22
23
24
sRNA size (nt)

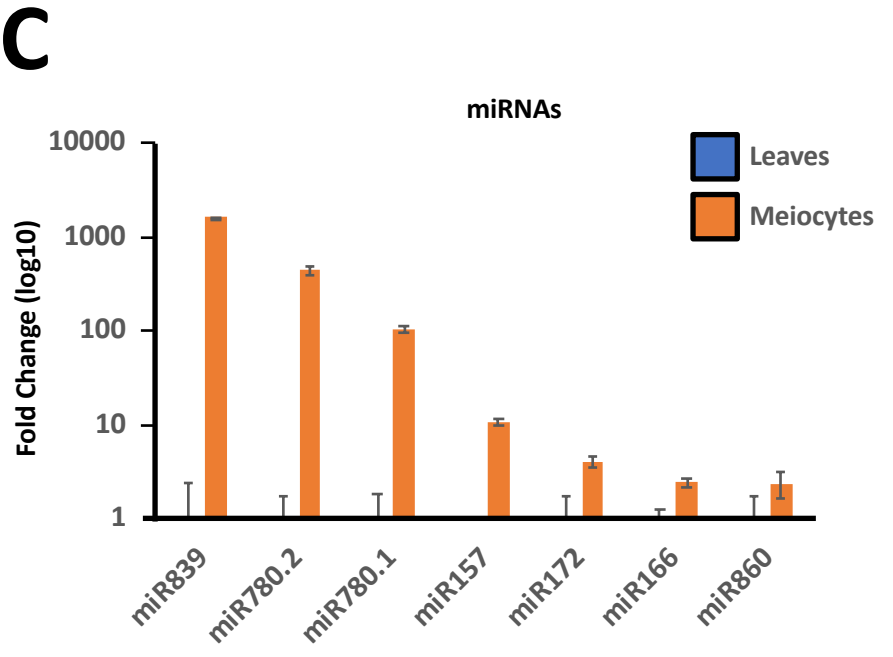
C
miRNAs
Leaves
Meiocytes
Fold Change (log10)
10000
1000
100
10
1
miR839
miR780.2
miR780.1
miR157
miR172
miR166
miR860

Figure 2.

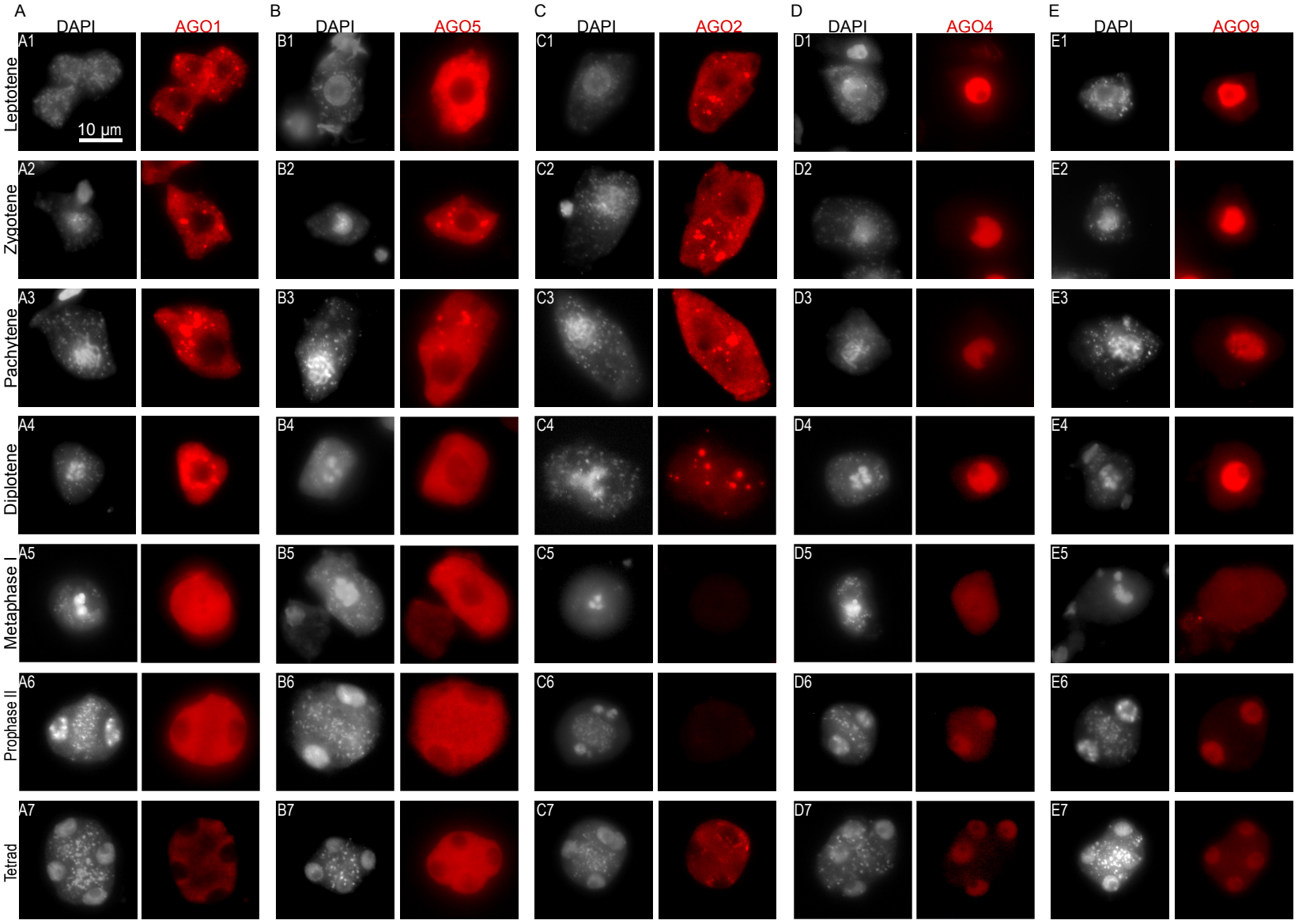
A
DAPI
AGO1
B
DAPI
AGO5
C
DAPI
AGO2
D
DAPI
AGO4
E
DAPI
AGO9
Leptotene
Zygotene
Pachytene
Diplotene
Metaphase I
Prophase II
Tetrad
A1
B1
C1
D1
E1
A2
B2
C2
D2
E2
A3
B3
C3
D3
E3
A4
B4
C4
D4
E4
A5
B5
C5
D5
E5
A6
B6
C6
D6
E6
A7
B7
C7
D7
E7
10 µm